JOURNAL OF MATERIALS SCIENCE **38** (2003) 2925–2934

Ageing characteristics of furnace cooled eutectoid Zn-Al based alloy

Y. H. ZHU*, H. C. MAN, H. J. DORANTES-ROSALES, W. B. LEE
Department of Industrial and Systems Engineering, The Hong Kong Polytechnic University, Hong Kong, People's Republic of China
E-mail: yaohuazhu@hotmail.com

Phase transformations and microstructural changes of a furnace cooled eutectoid Zn-Al based alloy were studied during ageing at 100 and 170°C using X-ray diffraction (XRD), scanning electron microscopy (SEM) and transmission electron microscopy (TEM) techniques. Three phase transformations occurred in the furnace cooled eutectoid Zn-Al alloy. The metastable η'_{FC} phase decomposed during isothermal ageing. The four-phase transformation, $\alpha + \varepsilon \rightarrow T' + \eta$ followed the discontinuous decomposition of the η'_{FC} phase. Typical morphologies of the decomposition of the η'_{FC} and ε phases were observed in scanning electron microscopy. Decomposition of Al-rich α phase was observed during the prolonged ageing by transmission electron microscopy. The different types of decomposition of the different metastable phases dominated at different stages of ageing.

1. Introduction

Slow cooling is common in cast ingot production. Phase transformation and microstructural change involved in the slow cooling process are much more complicated than solution treated-quenched alloy, and closely related with the properties of the cast ingot. It is of interest to study the structural evolution of an alloy during slow cooling and its relation with properties. Furnace cooling is a slow cooling process, which consists of two stages of heat treatments. The alloy is first solution treated at a high temperature for a period of time to reach equilibrium state at that temperature, and then followed by slow cooling to room temperature within the furnace. Various metastable phases are formed during furnace cooling, and decompose in subsequent isothermal treatment.

The present paper deals with the decomposition of various metastable phases and the related structural change in a furnace cooled eutectoid Zn-Al based alloy.

2. Experimental

A cast ingot of the eutectoid Zn-Al based alloy of composition Zn76-Al22-Cu2 (in weight) was solution treated at 350°C for 4 days and then furnace cooled to the room temperature.

The as furnace cooled (FC) alloy specimens were examined using both X-ray diffraction (XRD) and Scanning Electron Microscopy (SEM) to obtain overall views of the metallurgical structure and phase transformation prior to more detailed examination in the transmission electron microscope (TEM). X-ray diffraction examination was performed on flat polished specimen in the as FC state and at various stages of subsequent ageing at 100° and 170°C. The characteristic X-ray diffraction spectrum was collected within a range of diffraction angle 2θ from 35° to 47°, at a scanning speed of $1^\circ\,\text{min}^{-1}$ in a Philips X-ray diffractometer. Nickel-filtered Cu radiation was used. The tested specimens were ground and polished by standard techniques and examined by SEM in the as polished state using a backscattered electron detector to produce a medium resolution of good atomic contrast between the Aluminum-rich, Copper-rich and Zinc-rich phases in the alloy. Specimens for both XRD and SEM were duplicated. The relative intensity of X-ray diffraction of various phases involved was obtained by calculating the area of the characteristic diffraction peaks of the phases at various stage of ageing.

Thin disc specimens of 3 mm diameter for TEM work were prepared by wet grinding and punching the flat heat treated specimens and further wet grinding down to a thickness of about 100 μm. Thin foil specimens were finally produced using electropolishing in a double-jet electropolisher at a temperature below −40°C in a 20% perchloric acid/80% methanol solution. The thin foils were examined using JEOL 2000-FXII transmission electron microscope. Conventional TEM was used to produce high resolution images of both bright field and the dark field, and selected-area diffraction pattern (SADP).

* Author to whom all correspondence should be addressed.

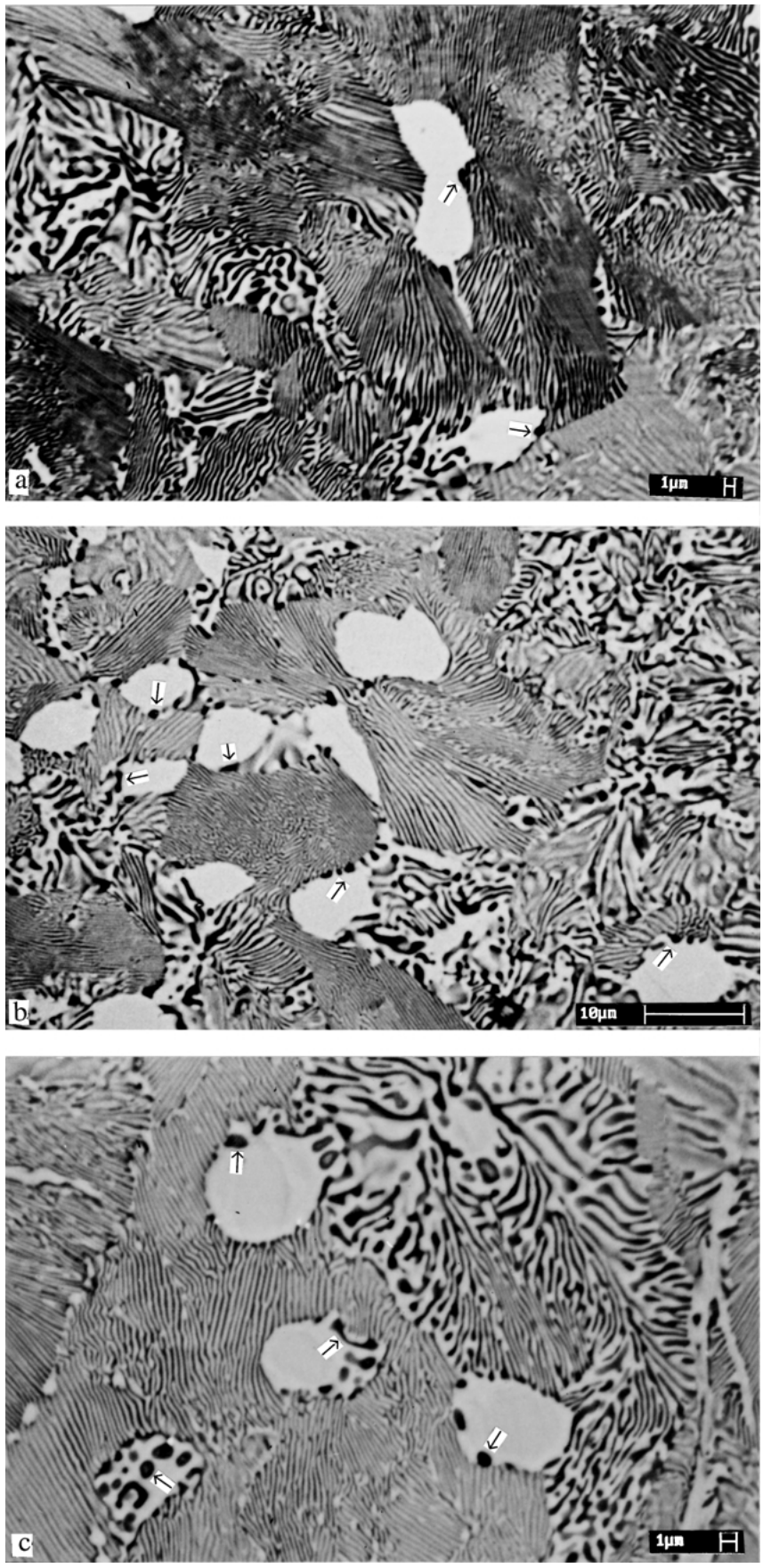

Figure 1 SEM Backscattered micrographs of the FC Zn-Al based alloy of as FC state (a) and after 10 hrs (b), and 30 hrs (c) of ageing at 100°C.

3. Results and discussion

3.1. Microstructure of the as FC eutectoid Zn-Al based alloy

In our previous publications [1, 2], it was reported that in the eutectoid Zn-Al based alloy (ZnAl22Cu2) there were only two phases β (Zn-rich phase of fcc structure) and ε (hcp Zn_4Cu) after being solution treated at 350°C for 4 days.

During furnace cooling, the β phase became an unstable β'_s phase and decomposed into various metastable

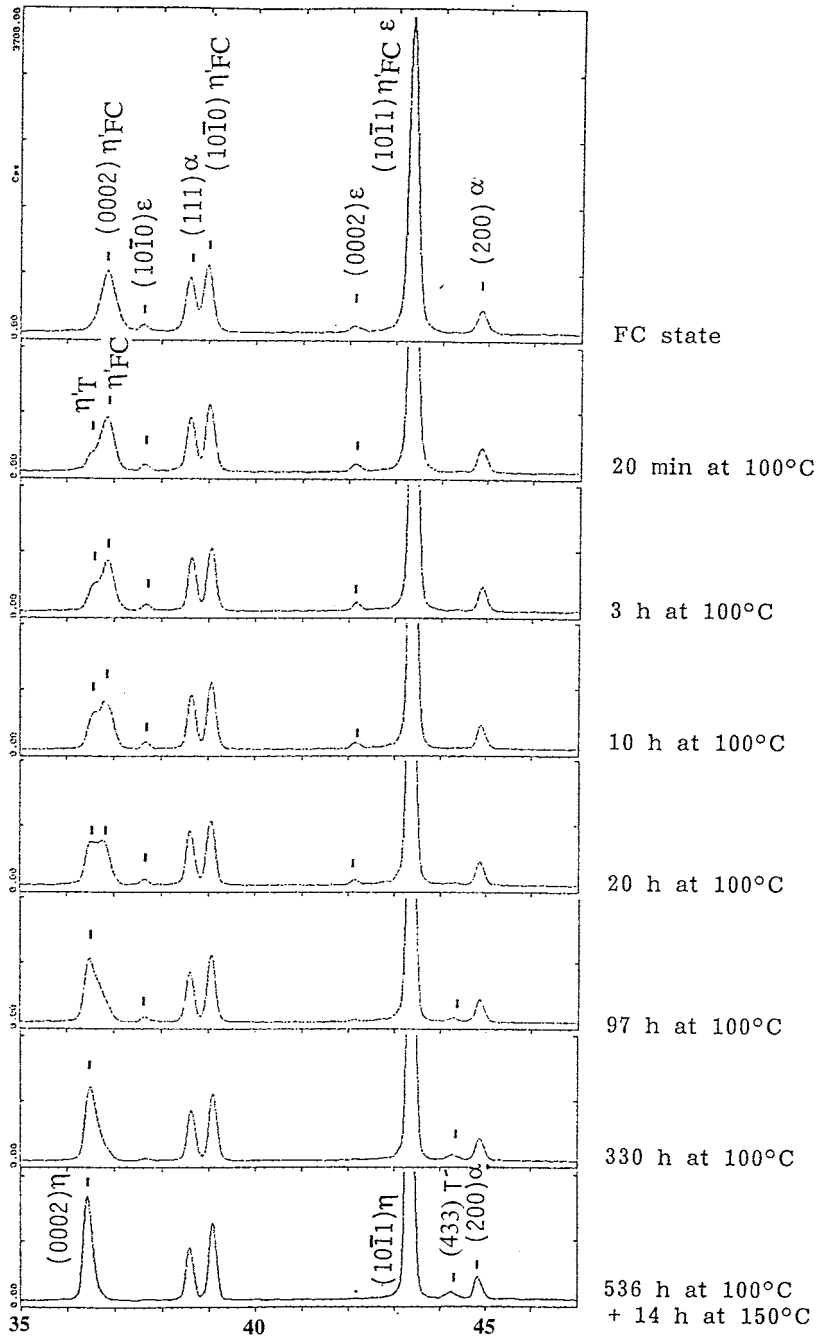

Figure 2 X-ray diffractograms of the FC Zn-Al based alloy of as FC state and after various stages of ageing at 100°C, showing two phase transformations.

phases. The various Al-rich and Zn-rich metastable phases decomposed into coarse lamellae and fine lamellae due to different diffusion rate of Al and Zn atoms. The ε phase did not decomposed in the as FC alloy specimen and appeared as the original particles. The resultant microstructure of the as FC alloy specimen consisted of coarse and fine lamellae, and the light contrast η'_{FC} (Zn-rich phase of hcp structure) and the ε phase particles, as shown in Fig. 1.

The as FC eutectoid Zn-Al based alloy consisted of three metastable phases α (fcc Al-rich phase), η'_{FC} and ε, as shown in the X-ray diffractograms in Fig. 2. Within the diffraction 2θ range of 37–47°, strong X-ray diffraction was observed for the various phases involved. The X-ray diffraction of the α phase from (111) and (200) appeared at 38.6° and 44.8°. The characteristic (0002) diffraction peak of η'_{FC} phase was at 2θ 36.8°. The (10$\bar{1}$0) and (0002) X-ray diffraction peaks of the ε phase were located at 37.6° and 42.1°. The (10$\bar{1}$1) diffraction peaks from the η'_{FC} phase and the ε phase overlapped at 2θ 43.3°.

The Al-rich α phase and the Zn-rich η'_{FC} phase in the lamellar microstructure were detected using TEM. The TEM bright field image of the fine lamellae is shown in Fig. 3a. The SADP was identified as from the [011] zone of the α phase. The SADP and the indexing of the diffraction pattern are shown in Fig. 3b and c. The dark field image using {200}α of the fine lamellae is shown in Fig. 3d. Located at grain boundaries in Fig. 3a are the ε phase particles, from which a diffraction pattern was identified from the [01$\bar{1}$1] zone of the hcp ε phase, as shown in Fig. 3e. Shown in Fig. 4 are the TEM bright

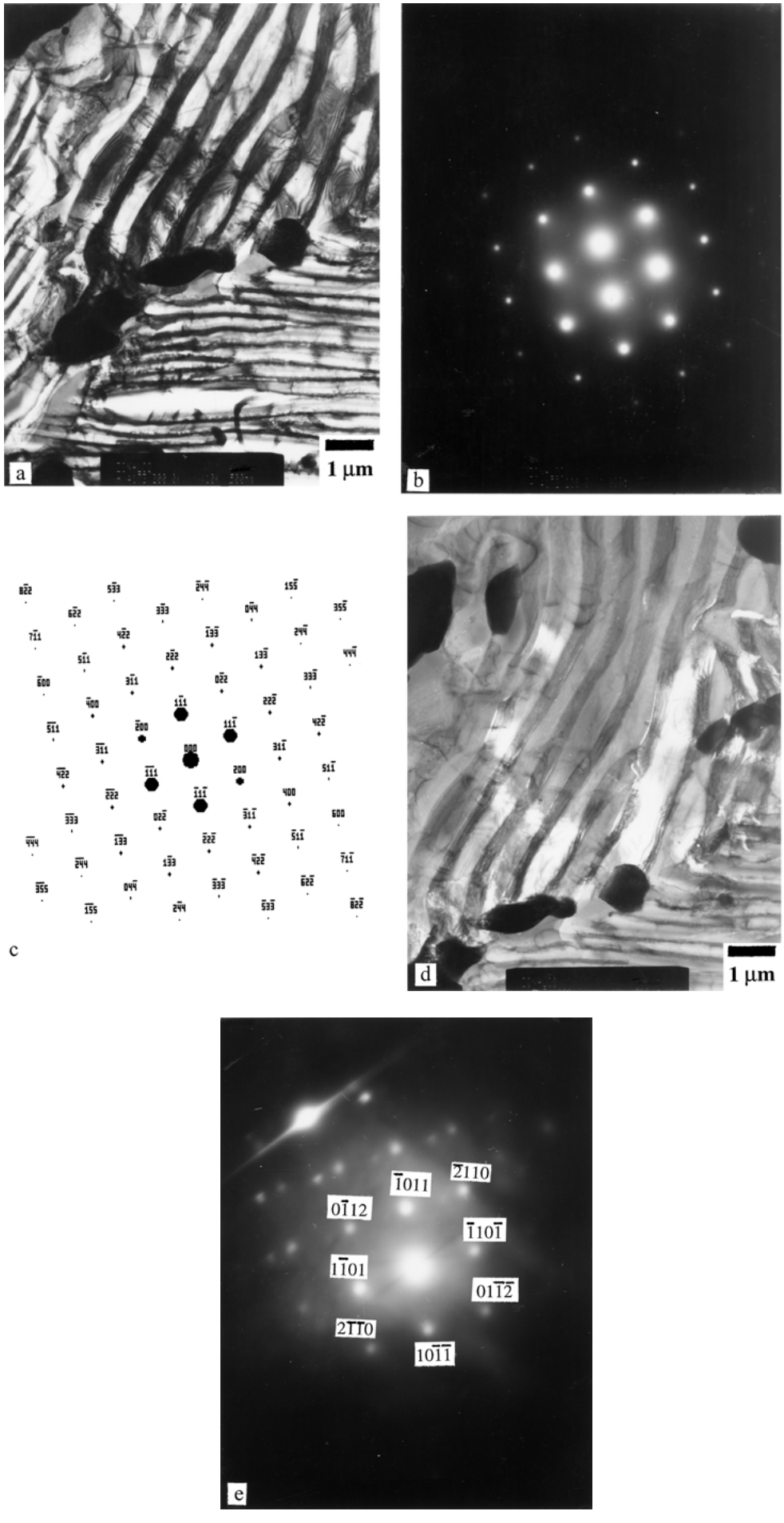

Figure 3 TEM bright field (a) of the fine lamellar structure in the as FC Zn-Al based alloy, the SADP from [011] zone of the α phase (b), the indexing of the diffraction pattern (c), dark field using $\{200\}\alpha$ (d), and the diffraction pattern from $[01\bar{1}1]$ zone of the ε phase particles located at the grain boundaries (e).

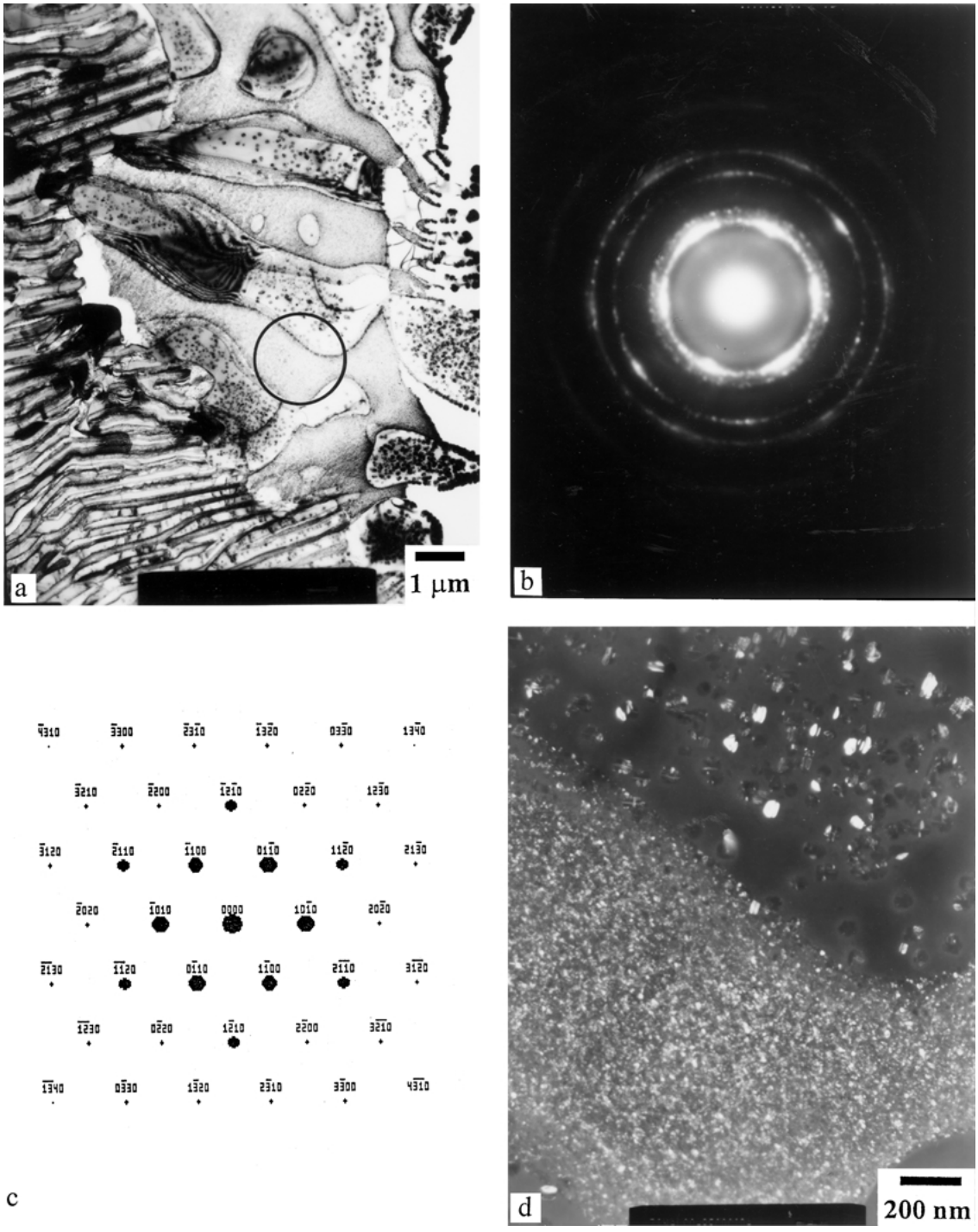

Figure 4 TEM bright field (a), the SADP from [0001] zone of the Zn-rich η'_{FC} phase (b) togehter with the indexing of the diffraction pattern (c) and the dark field from $\{0\bar{1}10\}\eta'_{FC}$ (d) of the as FC Zn-Al based alloy specimen.

field (a), the SADP from [0001] zone of the Zn-rich η'_{FC} phase (b) together with the indexing of the diffraction pattern (c) and the dark field from $\{0110\}\eta'_{FC}$ (d) of the as FC Zn-Al based alloy specimen.

In the as FC eutectoid Zn-Al based alloy specimen, several dark imaged particles of precipitates of Al-rich α phase were observed in the light imaged Zn-rich η'_{FC} phase as indicated by the arrow "→" in the SEM micrograph in Fig. 1a. Also the existence of precipitates of 40–50 nm in diameter was clearly detected inside the α phase using transmission electron microscopy, as shown in Fig. 4. The SADP (Fig. 4c) was identified as from [0001] zone of the η'_{FC} phase which was beside the metastable α phase in Fig. 4a. Therefore, the TEM dark field image (Fig. 4d) obtained from the $\{0\bar{1}10\}\eta'_{FC}$ in the SADP (Fig. 4c) shows the η'_{FC} phase precipitates in the α phase particle. The small amount of fine precipitates were not detected in the dark imaged Al-rich α phase using back scatter SEM.

3.2. Ageing characteristics

3.2.1. Decomposition of the η'_{FC} and ε phases

During ageing at 100°C, the precipitation of α phase in the η'_{FC} phase was further observed, as arrows pointed

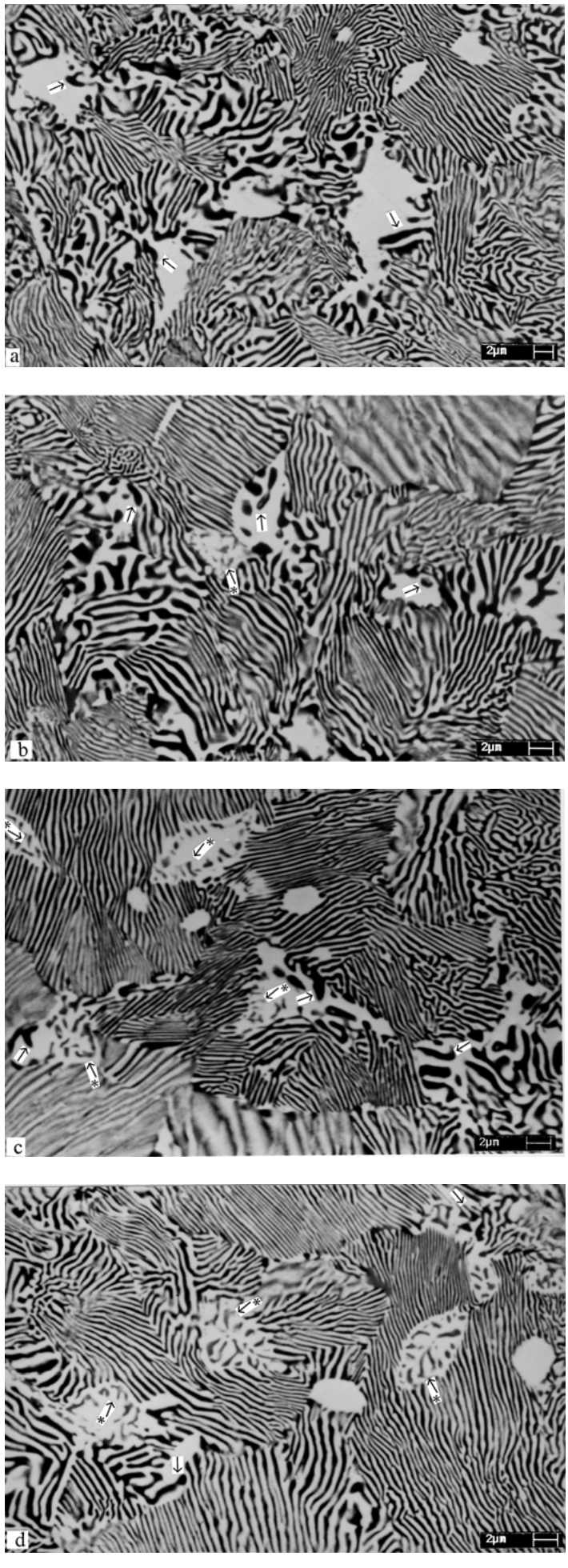

Figure 5 SEM Backscattered micrographs of the FC Zn-Al based alloy after various stages of ageing at 170°C: (a) 1 h (b) 10 h (c) 30 h, and (d) 52 h.

in Fig. 1. The dark imaged α phase precipitates grew at the phase boundaries (see after 10 h ageing at 100°C, Fig. 1b), and were clearly developed after 30 h ageing at 100°C, Fig. 1c. This discontinuous precipitation was detected using XRD, as shown in Fig. 2. It was observed that the (0002) diffraction at 36.8° in the as FC specimen, and the (0002) diffraction peak decreased in height, whilst a metastable η'_T phase appeared at lower 2θ, 36.5°, accordingly the d-spacing of the η'_{FC} and the η'_T phases were 0.2437 nm and 0.2456 nm respectively. Upon further ageing, the (0002) peak of the η'_{FC} phase decreased in height and that of the η'_T phase increased at the lower 2θ angle. After 20 h ageing at 100°C, the original (0002) peak of the η'_{FC} phase had decreased greatly, and the η'_T phase had formed instead, as shown in Fig. 2. The decomposition of the η'_{FC} phase occurred apparently during ageing as a discontinuous precipitation, as shown in Figs 1 and 2. This discontinuous precipitation was then followed by continuous precipitation. The (0002) X-ray diffraction peak shifted further to the lower 2θ angle, and finally reached 36.4°, accordingly the d-spacing was 0.2466 nm, when the final stable η phase formed.

In the previous publications, it was reported in detail that during various thermal and thermomechanical processes (such as ageing; tensile-, creep-, fatigue-deformation and mechanical milling etc.) the decomposition of the metastable Zinc-rich phases η'_s, η'_{FC} and η'_E in the cast, the FC and the extruded eutectoid Zn-Al based alloys respectively was characterized by shifting of (0002) X-ray diffraction to the lower 2θ angle from the original diffraction 2θ, accordingly increasing the d-spacing [3–9].

Another phase transformation was detected after 20 h ageing at 100°C. Both X-ray diffraction peaks from the $(10\bar{1}0)$ and (0002) crystal planes of the ε phase decreased in height relatively at $2\theta = 37.6°$ and $2\theta = 42.1°$, accompanying the increasing of the (433) diffraction peak of the T′ phase. It was recognized as a four-phase transformation, $\alpha + \varepsilon \rightarrow T' + \eta$, in the previous research publications [10–14].

These two kinds of phase transformation, i.e., decomposition of the η'_{FC} phase and the four-phase transformation were also observed in the specimen aged at 170°C using SEM and XRD techniques.

Shown in Fig. 5 are SEM micrographs of the FC eutectoid Zn-Al based alloy specimen at various stage of ageing at 170°C. After 1 h ageing at 170°C, the dark imaged α phase was observed as precipitates in the light imaged η'_{FC} phase, Fig. 5a. After 10 h ageing at 170°C, the gray precipitates of the T′ phase were observed in the light imaged Zn-rich ε phase, as indicated by arrow "*→" in the Fig. 5b. At the same time the precipitation of the α phase was developing during ageing. As one of the products of the four-phase transformation, $\alpha + \varepsilon \rightarrow T' + \eta$, the T′ phase contains less of the light Al element and more the heavy Cu than the α phase, and appears as the gray precipitate in the back scattered electron

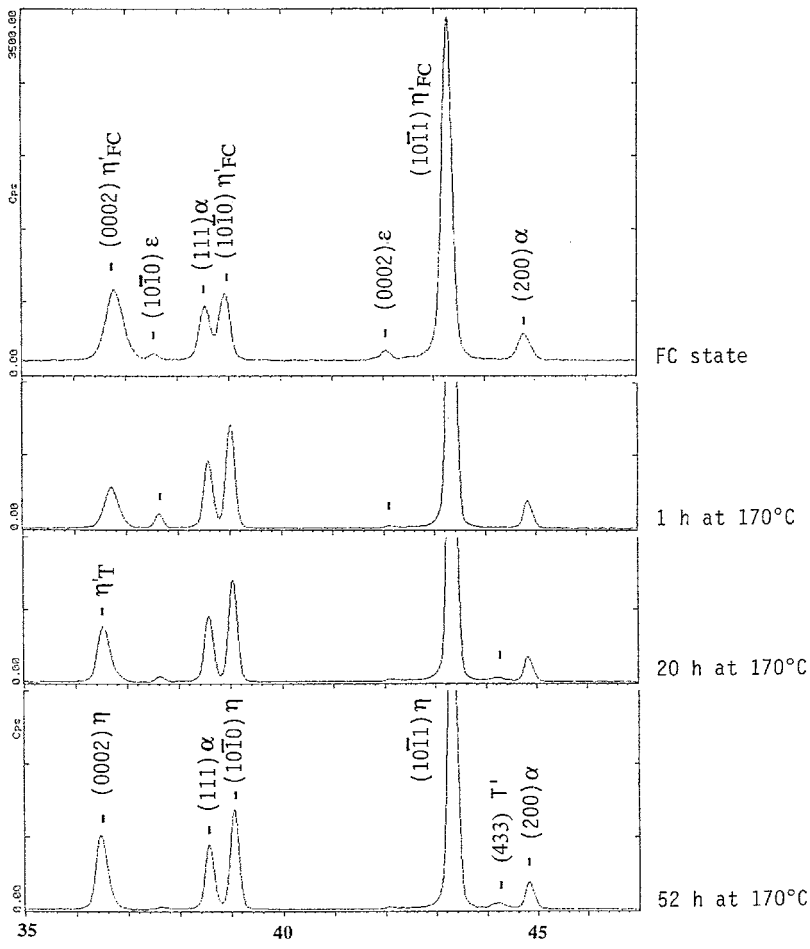

Figure 6 X-ray diffractograms of the FC Zn-Al based alloy of as FC state and after various stages of ageing at 170°C, showing two phase transformations.

image, being distinct from the dark imaged α phase precipitates in the η'_{FC} phase. Another product of the four-phase transformation, i.e., the η phase, posesses a similar atomic contrast with the ε phase, as both of the η and ε phases contain large amounts of the relatively heavy elements copper and zinc. This makes these two phases in distinguishable from one to another in the light imaged ε phase. Both precipitates of α phase and the T′ phase were apparently present after 30 h and 52 h ageing at 170°C, as shown in Figs 5c and d.

The X-ray diffractogram of the FC alloy specimen at various stages of ageing at 170°C is shown in Fig. 6. The characteristic shifting of the (0002) diffraction peak to the lower 2θ angle was also observed. It implied that the η'_{FC} phase decomposed during the early stage of ageing at 170°C. The change in diffraction intensity of both the ε and T′ phases was also observed during further ageing, as shown in Fig. 6. After 52 h ageing at 170°C, the $(10\bar{1}0)$ and (0002) diffraction peaks of the ε phase decreased greatly, whilst the (433) diffraction peak of the T′ phase increased in height. Compared with the XRD results at 100°C, Fig. 2, both phase transformations were apparently accelerated during ageing at 170°C, Fig. 6.

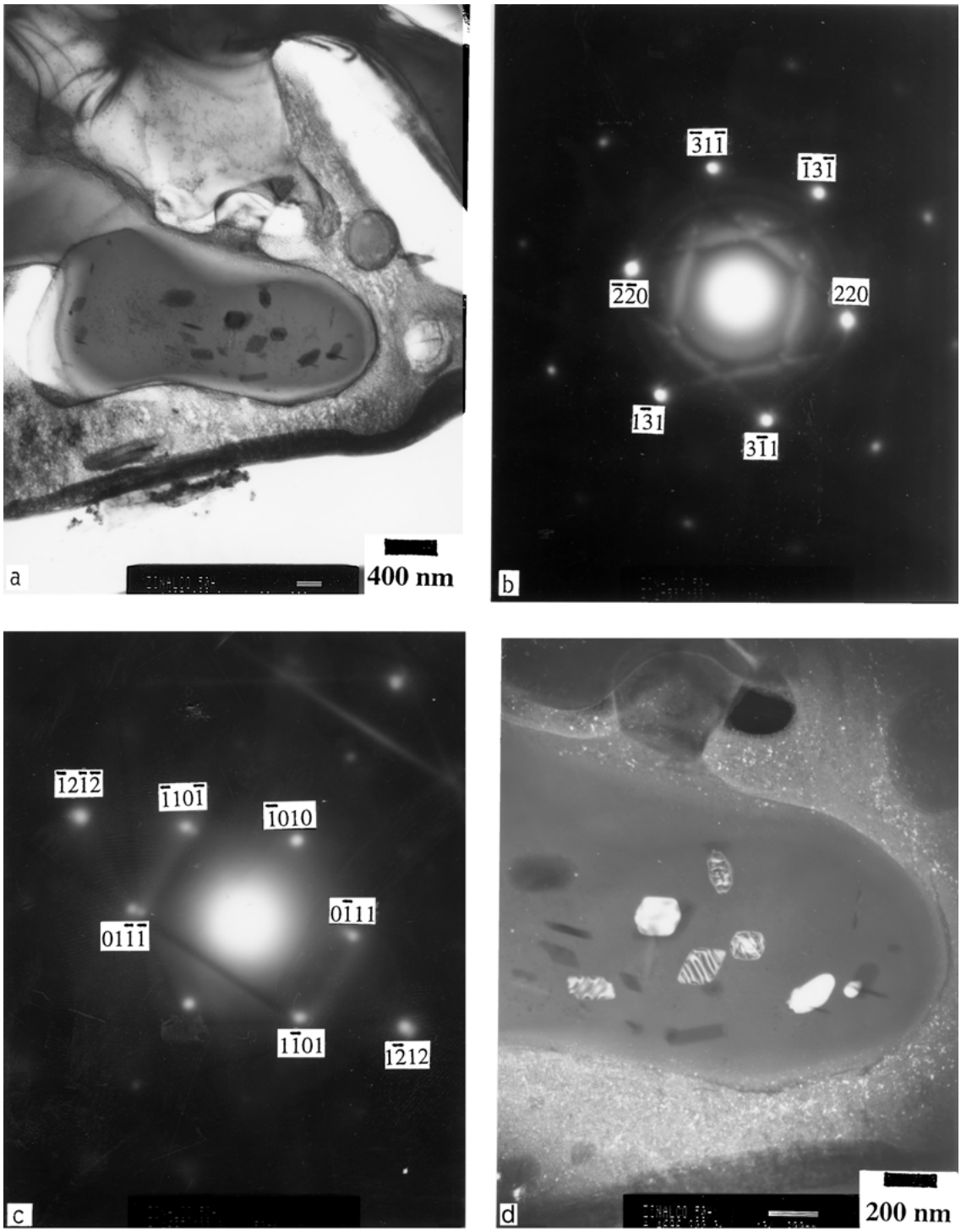

Figure 7 TEM bright field (a), the SADP from $[\bar{1}14]$ zone of the α phase particle (b) and the SADP from $[1\bar{2}1\bar{3}]$ zone of the precipitate η phase inside the α phase particle (c), and the dark field using $\{\bar{1}010\}\eta$ (d) for the FC Zn-Al based alloy specimen after 52 h ageing at 170°C.

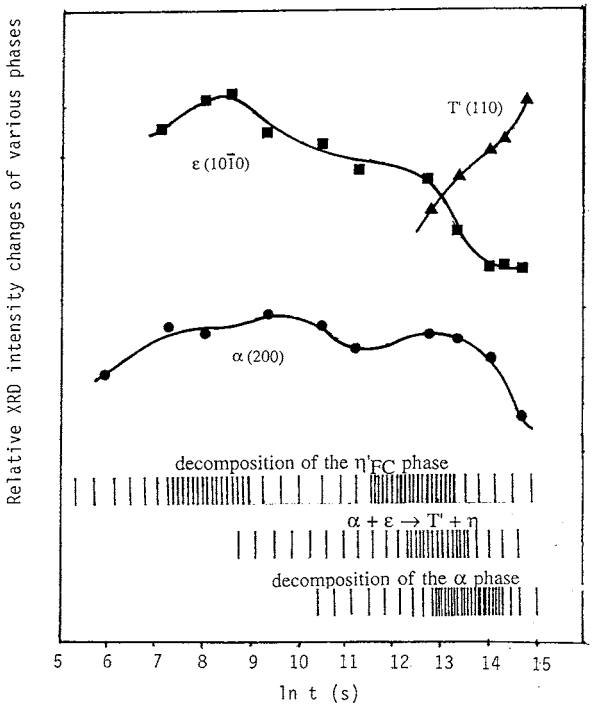

Figure 8 The relative XRD intensity changes of various phases in the FC eutectoid Zn-Al based alloy aged at 100°C.

3.2.2. Precipitation inside the α phase

Further decomposition of the α phase was detected during ageing at 170°C using TEM technique. According to the identification of the SADP, the precipitates inside the fcc α phase was hcp η phase. Shown in Fig. 7a is the TEM bright field of the FC Zn-Al alloy specimen after 52 h ageing at 170°C. A diffraction pattern from the particle in Fig. 7a is identified from the [$\bar{1}$14] zone of the fcc α phase, as shown in Fig. 7b. The SADP of the precipitate inside the α phase is identified from the [1$\bar{2}\bar{1}\bar{3}$] zone of the hcp η phase, as shown in Fig. 7c, and the dark field image using $\{\bar{1}010\}\eta$ is presented in Fig. 7d. In the TEM dark field image, Fig. 7d, the light image of the η phase precipitates inside the α phase particle is diffracted from $\{\bar{1}010\}\eta$ in the SADP, Fig. 7c. It was found that the precipitates of the η'_{FC} phase of 40–50 nm in diameter inside the α phase had grown to be the η phase of 80–100 nm in diameter after 52 h ageing at 170°C. Accordingly the Al-rich α phase in equilibrium with the η phase became the final stable α_f phase. This decomposition of the metastable α phase was detected for the first time during the prolonged ageing in the eutectoid Zn-Al based alloy. It is reasonable as the α phase in the FC Zn-Al based alloys, even after the four-phase transformation (a phase transformation correlated with a phase equilibrium, $\alpha + \varepsilon = T' + \eta$ at 268°C) is unstable. The α phase at 268°C contains more Zn in the Zn-Al based alloys compared with the composition of the α phase at 100° and 170°C, according to the phase diagrams of Zn-Al binary, Zn-Al-Cu ternary and Zn-Al-Cu-Si quaternary alloy systems [15–17]. There must be Zn-rich η phase precipitated from the unstable η phase at 100° and 170°C.

3.2.3. Relative XRD intensity changes of the various phases

The relative XRD intensity changes of the various phases α, ε and T′ at 100°C are plotted in Fig. 8. It is noticed that the relative XRD intensities of the α and ε phases increased in the early stage of ageing, accompanying the formation of the metastable phase η'_T. This implied that the η'_{FC} decomposed discontinuously into three phases, η'_T, α and ε: i.e., $\eta'_{FC} \rightarrow \eta'_T + \alpha + \varepsilon$. Following the discontinuous decomposition of the η'_{FC} phase, the relative XRD intensities of both the α and ε phases decreased during prolonged ageing. The latter decreasing of XRD intensities of both the α and ε phases was a consequence of the four-phase transformation, $\alpha + \varepsilon \rightarrow T' + \eta$, which is in agreement with the increasing of the T′ phases during prolonged ageing. Finally the XRD intensity of the α phase decreased, and this was attributed to the decomposition of the α phase.

It was clearly found that the types of decomposition of the different metastable phases dominated at different stages of ageing, which is indicated by shadowed solid lines and the greater line density means the faster the phase transformation rate would be, as shown in Fig. 8. The decomposition of the η'_{FC} phase occurred during the whole ageing processes. The discontinuous decomposition of the η'_{FC} phase, $\eta'_{FC} \rightarrow \eta'_T + \alpha + \varepsilon$, dominated at the early stage of ageing, as demonstrated by XRD intensities of the α and ε phases increasing, Then the four-phase transformation, $\alpha + \varepsilon \rightarrow T' + \eta$, started, and was associated with decreasing of the XRD intensities of the α and ε phases and increasing of the XRD intensity of the T′ phase. On further ageing the decomposition of the metastable η'_T phase became important and the XRD peaks of the α and ε phases increased slightly. Finally the decomposition of the α phase dominated the phase transformation, while the other metastable phases had almost decomposed completely, and the XRD intensity of the α phase decreasing significantly.

4. Conclusions

Three phase transformations occurred in the furnace cooled eutectoid Zn-Al based alloy (ZnAl22Cu2) during ageing at 100° and 170°C

(a) The metastable Zn-rich η'_{FC} phase decomposed throughout the ageing treatment. It decomposed first by discontinuous precipitation, $\eta'_{FC} \rightarrow \eta'_T + \alpha + \varepsilon$. The precipitation of the dark imaged Al-rich α phase was clearly observed using SEM backscttered electron imaging. This was followed by a continuous decomposition of the metastable η'_T phase, the (0002) X-ray diffraction peak shifting to a lower 2θ angle.

(b) Decomposition of the ε phase appeared as a four-phase transformation, $\alpha + \varepsilon \rightarrow T' + \eta$. The gray T′ phase precipitate was observed in the light contrast ε phase in the SEM.

(c) Decomposition of Al-rich α phase occurred during ageing. The precipitation of the η phase inside the α phase was clearly observed using TEM examination.

The different types of decomposition of the various metastable phases dominated at different stages of ageing.

Appendix

The X-ray diffraction intensity changes of various phases in the FC eutectoid Zn-Al based alloy aged at 100°C

t	lnt (s)	ε $2\theta = 37.6$ $(10\bar{1}0)$	42.1 (0002)	α 44.85 (200)	T′ $2\theta = 44.28$ (433)
FC				346.5	
5 m	5.70			368.5	
20 m	7.09	171.0	180.0	384.3	
45 m	7.90	182.0	190.0	383.0	
1.5 h	8.59	188.0	198.0	370.0	
3 h	9.29	167.2	192.0	396.0	
10 h	10.49	174.8	167.0	390.3	
20 h	11.18	158.9	150.0	379.8	
97 h	12.74	153.1	118.0	386.7	147.2
170 h	13.34	130.8	111.7	382.4	152.8
330 h	13.99	114.0		375.0	163.4
460 h	14.32	111.0		385.9	168.0
536 h	14.47	114.8		352.0	184.0

Acknowledgment

The authors are grateful to DGAPA de UNAM (Project No. IN503797) and The Research Committee of the Hong Kong Polytechnic University (Project No. G-YY26), also to L. Baños, A. Caballero and J. Guzman for their help on the experimental work.

References

1. Y. H. ZHU, H. C. MAN and W. B. LEE, *Mater. Sci. Eng. A.* **268** (1/2) (1999) 147.
2. Y. H. ZHU and H. C. MAN, *J. Mater. Sci. Lett.* **17** (1998) 111.
3. Y. H. ZHU, in Proc. 3rd International Conf. on Zn-Al Alloys, edited by G. Torres, Y. H. Zhu and C. Piña Barba, Mexico, 1994, p. 77.
4. Y. H. ZHU and F. E. GOODWIN, *J. Mater. Res.* **10**(8) (1995) 1927.
5. Y. H. ZHU and E. OROZCO, *Metall. & Mater. Trans.* **26A** (1995) 2611.
6. Y. H. ZHU and J. TORRES, *Zeit. Metallkunde*, **88** (1997) 329.
7. Y. H. ZHU, E. OROZCO and J. TORRES, *Mater. Trans. JIM* **38**(6) (1997) 521.
8. Y. H. ZHU and J. TORRES, *J. Mater. Proc. Techonol.* **73**(1–3) (1998) 25.
9. Y. H. ZHU, V. M. LOPEZ HIRATA and M. SAUCED MUÑOZ, *Zeit. Metallkunde* **88** (1997) 934.
10. R. CIACH, J. KROL and K. WEGRZYN-TASIOR, *Bull. Acad. Polon. Sci. (Techn.)* **17** (1969) 371.
11. J. KROL and K. WEGRZYN-TASIOR, *Arch. Hutn* **16** (1971) 199.
12. R. CIACH, B. DUKIET-ZAWEDZKA and T. D. CIACH, *J. Mater. Sci.* **13** (1978) 2676.
13. K. LOHBERG, *Zeit. Metallkunde* **74** (1983) 456.
14. N. MYKURA, S. MURPHY and Y. H. ZHU, *Proc. Mater. Res. Soc.* **21** (1984) 841.
15. A. A. PRESNYAKV, Y. A. GOTBAN and V. V. CHERPYAKOVA, *Russian Liter. on Phys. Chem.* **35** (1961) 623.
16. S. MURPHY, *Zeit. Metallkunde* **71** (1980) 96.
17. Y. H. ZHU and S. MURPHY, *Chin. J. Metal Sci. & Technol.* **2** (1986) 105.

Received 29 May 2002
and accepted 22 April 2003